

Supporting information

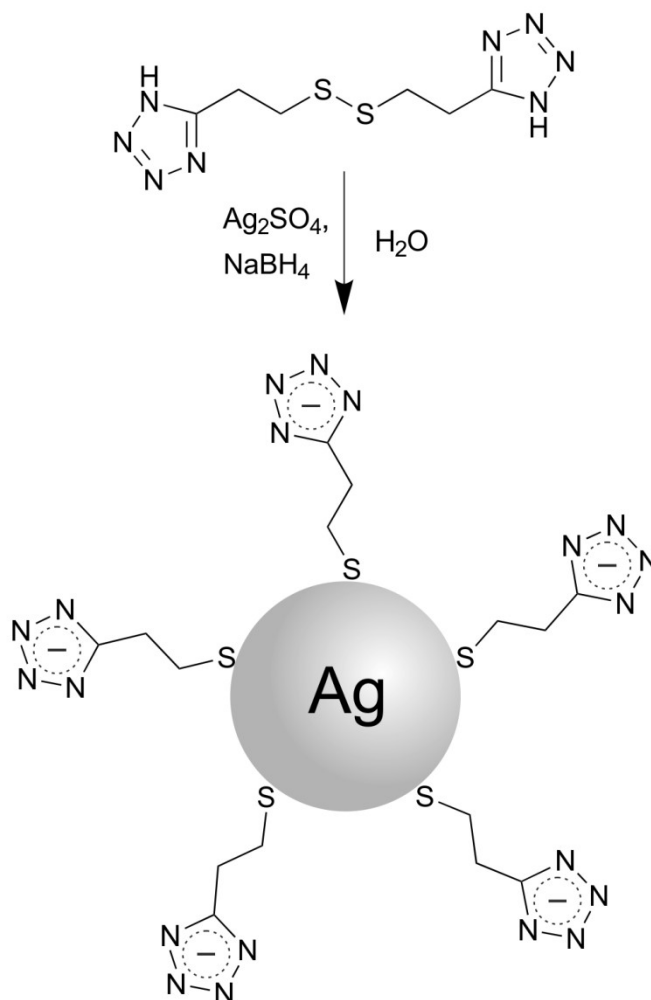


Figure S1. Scheme for the synthesis of tz-Ag NPs

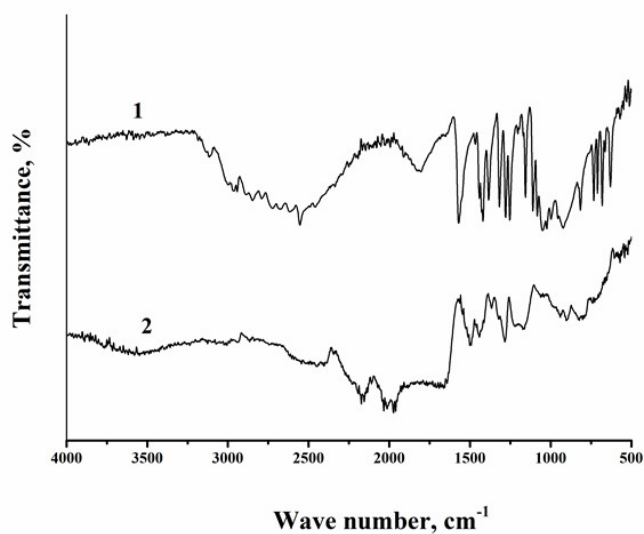


Figure S2. IR spectra of 5-(2-mercaptoethyl)tetrazole (1) and Ag NPs stabilized with 5-(2-mercaptoethyl)tetrazole (2)

IR spectra indicate that 5-(2-mercaptoethyl)tetrazole acts as a stabilizer for silver particles. The interaction between the particle surface and the ligand occurs due to the formation of a sulfur-silver bond, as indicated by the disappearance of the doublet of the sulfur-hydrogen bond line at 2556 cm^{-1} . The absence of NH modes at 1286 cm^{-1} and 1297 cm^{-1} indicates deprotonation of nitrogen atom in the ring, and hence the tetrazole ring is negatively charged [1].

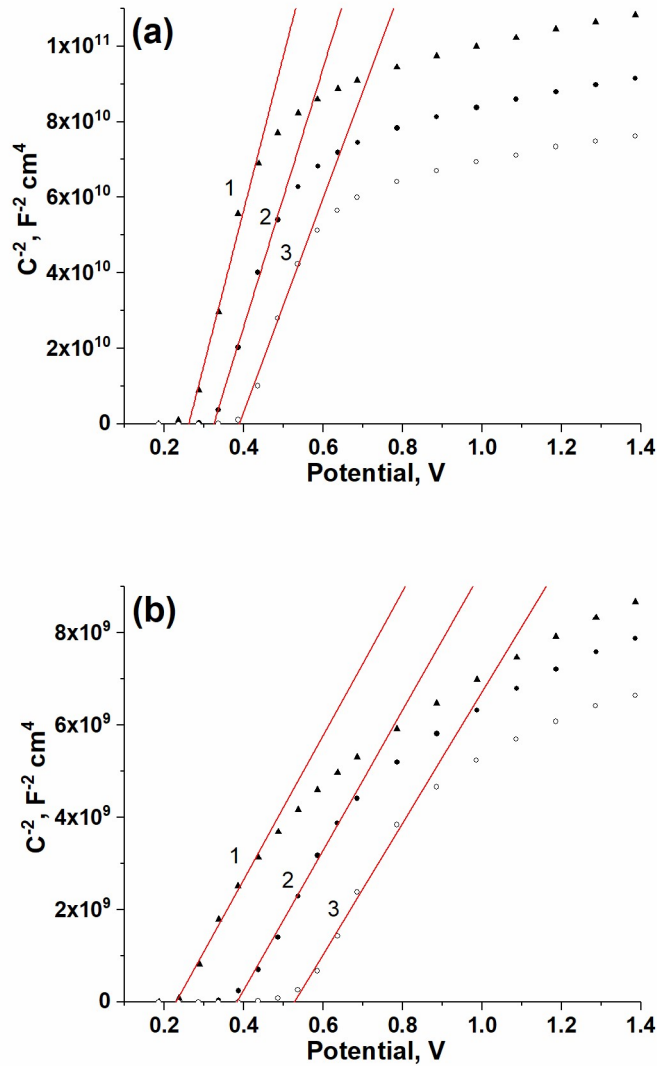


Figure S3. Mott-Schottky plots obtained for the TNT electrodes annealed at 500°C in air (a) and in a hydrogen atmosphere (b). Impedance measurements were carried out at frequencies of 1000 Hz (1), 100 Hz (2) and 10 Hz (3)

The concentration of defect states (N_d) for the TNT electrodes can be obtained from the Mott-Schottky relation [2]:

$$C_{SC}^{-2} = \left(\frac{2}{\epsilon\epsilon_0 e N_d S^2} \right) \left(E - E_{fb} - \frac{kT}{e} \right), \quad (1)$$

where C_{sc} is the differential capacitance of the space charge layer, S the electrode surface, E the applied potential, E_{fb} the flatband potential, k the Boltzmann's constant, e the electron charge, ϵ_0 the vacuum permittivity, ϵ the relative permittivity, N_d the ionized donor density and T the absolute temperature.

The value of the relative permittivity was 57 [3–5].

From the slope of the linear part of the C_{sc}^{-2} vs. E at negative potentials the ionized donor density (N_d) can be calculated, which was $6.05 \times 10^{18} \text{ cm}^{-3}$ for TNT layers heated in air, and $1.43 \times 10^{20} \text{ cm}^{-3}$ for TNT layers heated in hydrogen (Figure S3). The obtained data confirm the fact that TNT layers after annealing in H_2 atmosphere have a noticeably higher concentration of defects compared to TNT heated in air.

The preparation of the compact TiO_2 electrode

The compact TiO_2 films were obtained by thermal oxidation of titanium electrodes, as well as by hydrolysis of polybutyltitanate. Thermal oxidation of titanium substrates was carried out in air at $450 \text{ }^\circ\text{C}$ for 3 hours. The heating rate during the oxidation process was $5 \text{ }^\circ\text{C}$ per minute. The thickness of the films obtained by thermal oxidation was 50 nm.

Thin non-porous TiO_2 films were also produced by sol-gel technique. In this case, polished titanium plates were immersed for a short time in 1 wt. % solution of polybutyltitanate in tert-butanol, dried in air (during the drying process, hydrolysis of polybutyltitanate occurred with the participation of moisture from the air) and then heated at $200 \text{ }^\circ\text{C}$ for 20 min. To obtain films with a thickness of 50-100 nm, the cycle was repeated 3 times. Finally, the samples were heated at a temperature of $450 \text{ }^\circ\text{C}$ for 1 h to form a crystalline (anatase) structure.

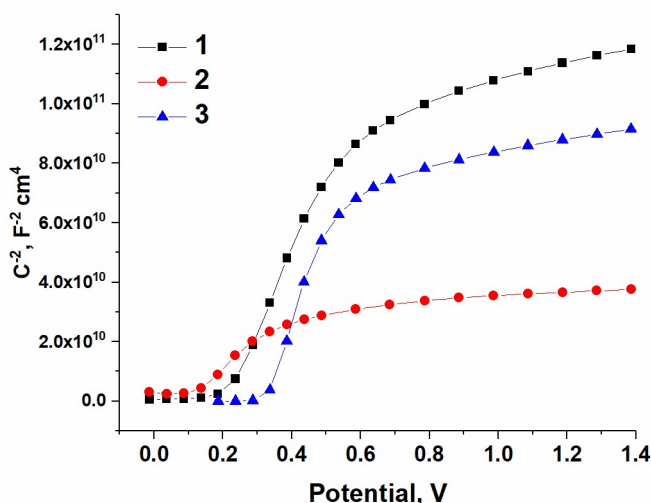


Figure S4. Mott-Schottky plots obtained for the compact TiO_2 films produced by sol-gel technique (1) and thermal oxidation (2), and for TNT electrodes (3)

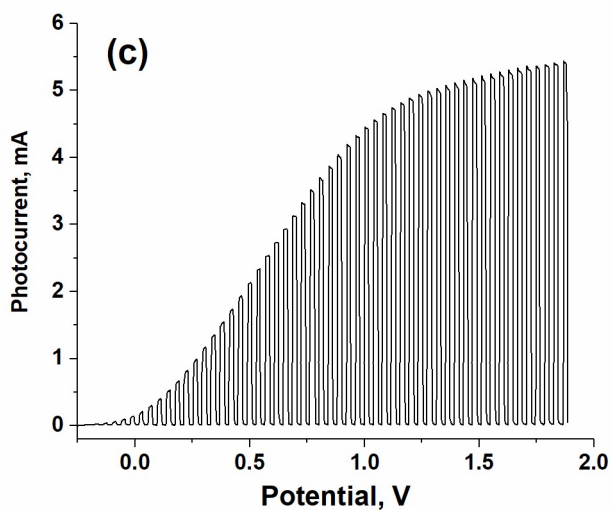
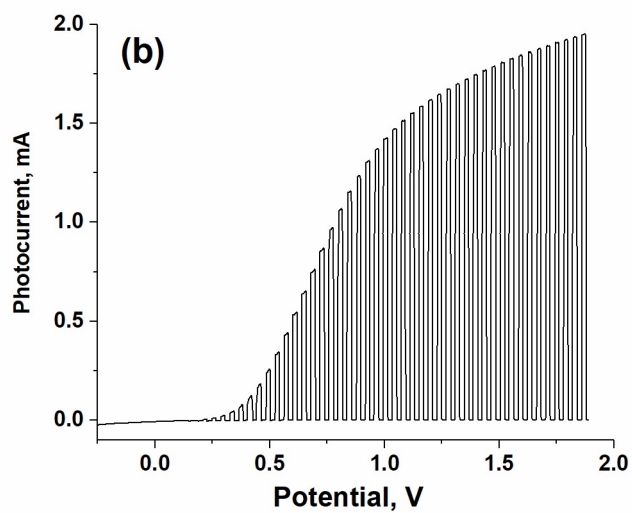
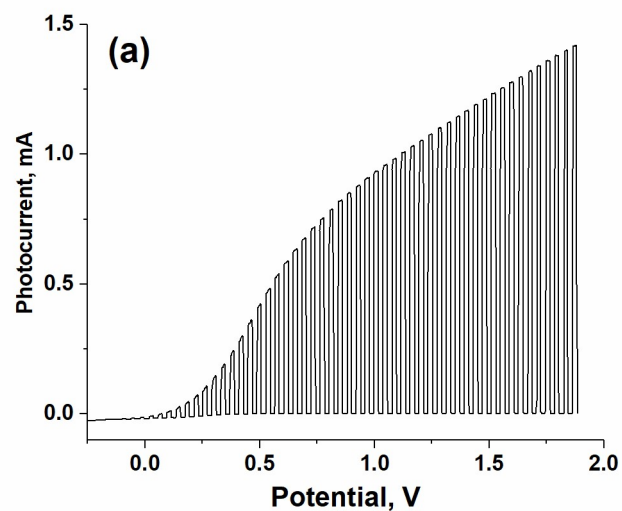


Figure S5. Current-potential curves recorded under chopped illumination for the compact TiO₂ electrodes prepared by thermal oxidation (a) and sol-gel technique (b), and for TiO₂ nanotubes annealed in air (c)

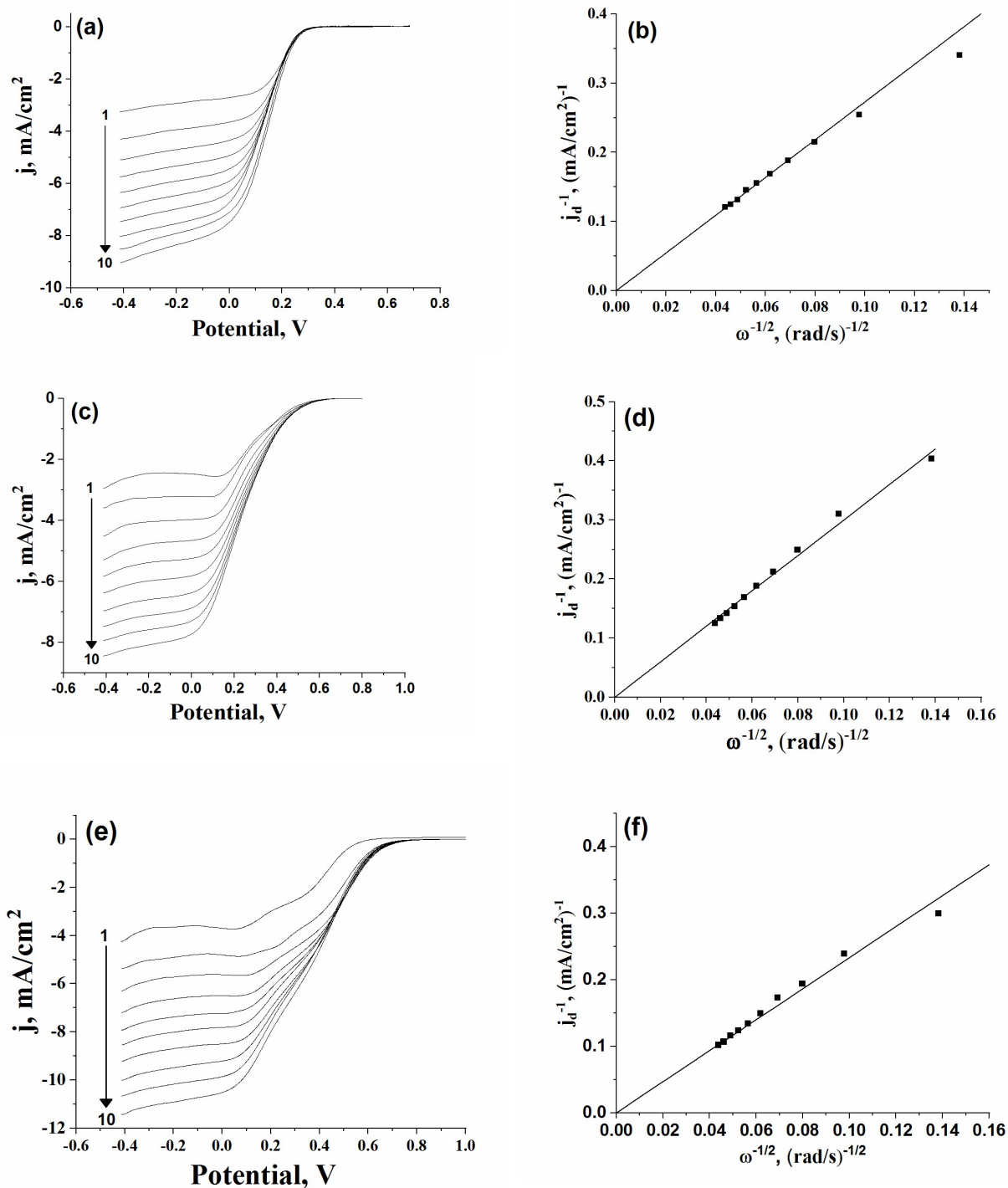


Figure S6. The voltammograms (a, c, e) of ORR for various rotation rates (1 – 500 rpm; 2 - 1000 rpm; 3 - 1500 rpm; 4 - 2000 rpm; 5 - 2500 rpm; 6 - 3000 rpm; 7 - 3500 rpm; 8 - 4000 rpm; 9 – 4500 rpm; 10 - 5000 rpm) and Koutecky-Levich plots ($E = -0.3$ V) (b, d, f) obtained on TNT (a, b), hTNT (c, d) and tz-Ag NPs/hTNT (e, f) in an O₂-saturated 0.1 M KOH

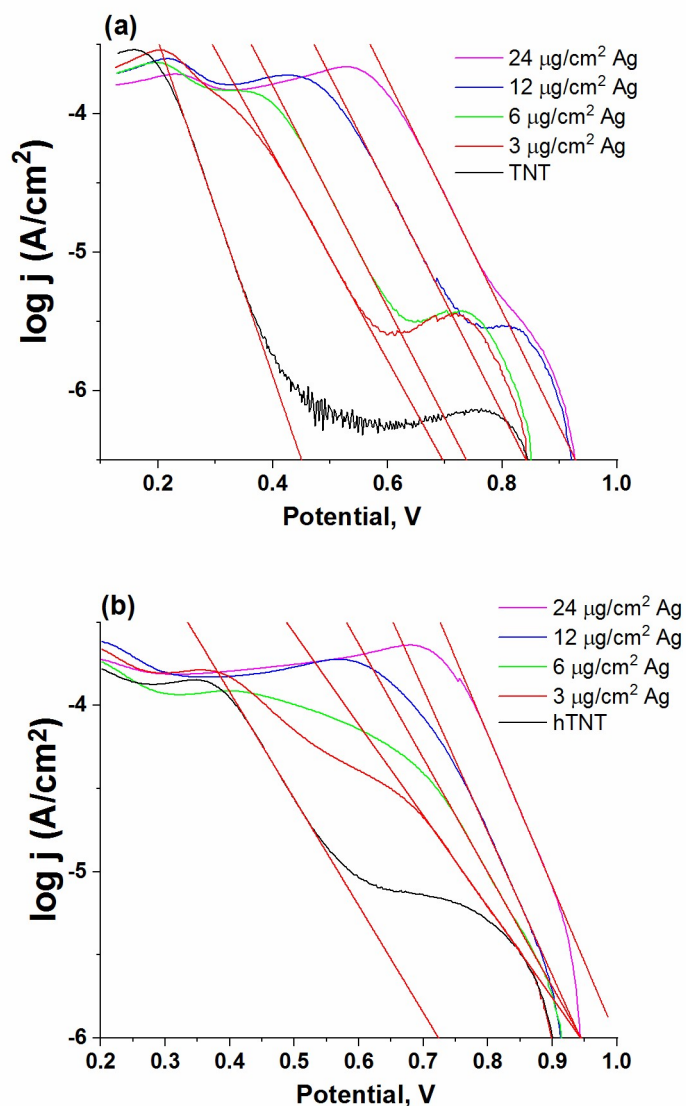


Figure S7. Tafel plots for O_2 electroreduction on tz-Ag NPs/TNT (a) and tz-Ag NPs/hTNT electrodes (b), and on bare TNT (a) and hTNT electrodes (b). Data derived from Fig.5.

The silver wire was soaked in 10 mL of aqueous solution containing 10 mM 5-(2-mercaptoethyl)tetrazole and 0.1 M KOH for 1h. The tz-adsorbed electrode was transferred to O_2 -saturated 0.1 M KOH solution for electrochemical measurements. Electrochemical experiments were performed in a single-compartment glass cell with a standard three-electrode configuration. An Hg/HgO electrode filled with 1 M KOH (Radiometer Analytical) and a Pt foil were used as the reference and counter electrodes, respectively.

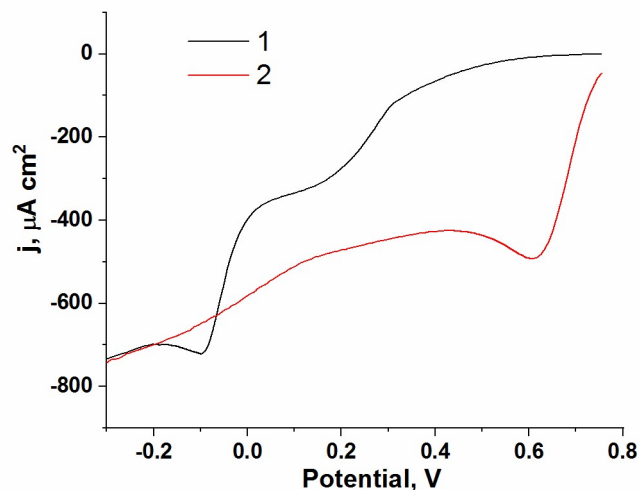


Figure S8. Voltammograms of ORR in an oxygen-saturated 0.1 M KOH solution recorded for bulk Ag electrode after adsorption of 5-(2-mercaptoethyl)tetrazole (1 – 1st scan; 2 – 2nd scan)

References

- [1] S. Thomas, N. Biswas, S. Venkateswaran, S. Kappor, S. Naumov, T. Mukherjee Studies on Adsorption of 5-amino Tetrazole on Silver Nanoparticles by SERS and DFT Calculations / J. Phys. Chem. A 2005, 109, 9928 – 9934.
- [2] P. Schmuki, H. Böhni, J.A. Bardwell, *In Situ* Characterization of Anodic Silicon Oxide Films by AC Impedance Measurements / J. Electrochem. Soc. 1995, 142, 1705–1712. doi: [10.1149/1.2048644](https://doi.org/10.1149/1.2048644)
- [3] S. Piazza, L. Calà, C. Sunseri, F. Di Quarto, Influence of the crystallization process on the photoelectrochemical behaviour of anodic TiO₂ films, Ber. Bunsenges. Phys. Chem. 1997, 101, 932–942. doi: [10.1002/bbpc.19971010608](https://doi.org/10.1002/bbpc.19971010608)
- [4] D.J. Blackwood, L.M. Peter, The influence of growth rate on the properties of anodic oxide films on titanium, Electrochim. Acta 1989, 34, 1505–1511. doi: [10.1016/0013-4686\(89\)87033-1](https://doi.org/10.1016/0013-4686(89)87033-1)
- [5] M. Schneider, S. Schroth, J. Schilm, A. Michaelis, Micro-EIS of anodic thin oxide films on titanium for capacitor applications, Electrochim. Acta 2009, 54, 2663–2671. doi: [10.1016/j.electacta.2008.11.003](https://doi.org/10.1016/j.electacta.2008.11.003)